

## Increasing the efficiency of photovoltaic cells based on Kazakhstan silicon

I. Klinovitskaya<sup>1\*</sup>, D. Kalygulov<sup>1</sup>, S. Plotnikov<sup>1</sup>, P. Lay<sup>2</sup>

<sup>1</sup>*D. Serikbayev East Kazakhstan Technical University, The Faculty of Energy, 69 Protozanov Street, 070004, Ust-Kamenogorsk, The Republic of Kazakhstan, [iklinovitskaya@inbox.ru](mailto:iklinovitskaya@inbox.ru)*

<sup>2</sup>*ECM Technologies, 46 rue Jean Vaujany – Technisud, F-38029 Grenoble, France*

The study of the solar cells properties is a relevant topic since development of solar energy meets the global demand and complies with the policy of the Government of the Republic of Kazakhstan on its transition to a "green" economy. Various properties of solar cells such carrier lifetime, reflectivity, and quantum efficiency affect the efficiency of solar cells directly. This study is devoted to obtaining and comprehensive study of solar cells manufactured on the basis of the Kazakhstan multicrystalline silicon of solar grade. The study applied: a method of microwave detected photoconductive decay ( $\mu$ -PCD), a method of Light Beam Induced Current (LBIC), methods for spectrometric analysis of reflection, transmission and photoluminescence coefficients, scanning electron microscopy, and methods for analyzing current-voltage characteristics. Al BSF and PERC solar cells based on Kazakhstan silicon have been produced and analyzed. The study proposes modification of the standard Al-BSF line to the PERC line.

**Keywords:** solar cells, crystalline silicon, Al-BSF structure, PERC structure, solar energy

### INTRODUCTION

Photovoltaic (PV) energy conversion is predicted to play an important part in the future power market, and the interest in this technology is increasing worldwide. Our need for energy will continue to rise, as The United Nations predict the world population growth from 7.7 billion today to 9.2 billion by 2040 [1]. In that regard, the global energy consumption will increase by 28% [2]. Solar energy is the most important and powerful source of energy available to humanity.

Crystalline silicon (c-Si) PV cells are the most common solar cells, accounting for about 90% of the total PV market share. This technology provides the highest energy conversion efficiencies of all commercial solar cells and are expected to continue to play a primary role in the future of PV market.

As part of the transition to a "green" economy, in 2010, Kazakhstan began to implement a project for the production of photovoltaic modules based on the Sarykol quartz deposit. The subject of the research is solar cells production.

The aim of this study is to investigate the properties, possible optimization strategies to achieve high-efficiency solar cells with advanced architecture. Investigation of properties makes it possible to identify the existing reasons for the decrease in the efficiency of solar cells and to determine methods for its improvement.

### STANDARD BACK SURFACE FIELD (BSF) CELL ARCHITECTURE AND TECHNOLOGY

The standard BSF cell production technology includes several steps such as surface texturing, p-n junction creation by diffusion, emitter etching and phosphorus silicate glass (PSG) removal, antireflection coating (ARC) depositing by plasma-enhanced chemical vapor deposition (PECVD), metallization by screen-printing and firing. An overview of Standard Al BSF cell is given in Fig.1.

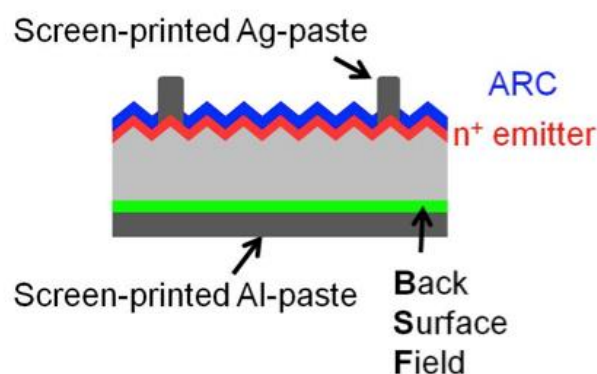


Fig.1. Standard Al BSF cell

Kazakhstan Solar Silicon LLP has implemented traditional production route of multicrystalline silicon (mc-Si) solar cells.

After wafering saw damages are removed and surfaces is normally textured in order to enhance light absorption. The next part of the fabrication is to form the p-n junction of the wafers. The substrate is p-type, so the junction is prepared by

\* To whom all correspondence should be sent:  
[iklinovitskaya@inbox.ru](mailto:iklinovitskaya@inbox.ru)

high-temperature diffusion of the n-type dopant, phosphorus, into the top surface. The dopant is deposited by exposure to nitrogen gas bearing phosphoryl chloride ( $\text{POCl}_3$ ) at high temperature [3]. The front surface of the wafer is further textured to reduce reflectivity, by depositing an anti-reflection coating (ARC). Traditional ARC is silicon nitride ( $\text{SiN}_y$ ) or titanium oxide ( $\text{TiO}_2$ ). Introducing a highly doped region near the back contact will increase  $I_{sc}$  and  $V_{oc}$ , and the effect is called a back surface field (BSF). This is a way to accomplish low effective recombination [4]. The most efficient technique to produce the BSF has proved to be to screen print an aluminium-based paste onto the rear of the cell and alloy the aluminium into the silicon by a firing process. The last step of the cell fabrication is adding front and back metal contacts.

As is well known, the solar cell industry is facing constant pressure to optimize their cell manufacturing processes, aiming higher efficiencies while not increasing costs significantly.

While in the past most research aimed at increasing the efficiency of solar cells was carried out on the front (sunny) side of the cell, recently the PV industry has shifted its focus to the rear (back) side. Or to be precise, today it is a lot about passivating the rear surface of a solar cell and accordingly modifying the metallization scheme. These rather simple changes adapted to standard solar cell processing entitle the produced silicon slices for a new name – PERC, which stands for Passivated Emitter and Rear Cell. Global trends and the power of energy produced in 2016-2020 are also shifting towards PERC technology. As it was noted in [5], about 50% of all the produced "solar" energy by 2020 would have been attributed to the PERC.

#### PASSIVATED EMITTER AND REAR CELL (PERC) CELL ARCHITECTURE AND TECHNOLOGY

PERC is gradually becoming the most cost-efficient choice for mass production of cells, and offers a good approach to surpass the 20% cell efficiency level in mass production [6].

An overview of PERC structure is given in Fig.2. Although the conversion to the PERC structure only requires that a few pieces of equipment are added to the standard production line, the improvement of efficiency is not an absolute [6]. Both the emitter and the rear of the cell have to be redesigned because improving only

one of them will not increase the cell efficiency as the recombination losses at the other device part will dominate. Further, if both emitter and rear surface are improved, recombination in the base region becomes important. This is due to boron-oxygen complex formation, which will suppress the FF in the cell. This means that PERC design requires a finetuning of influencing parameters that are not linearly interrelated.

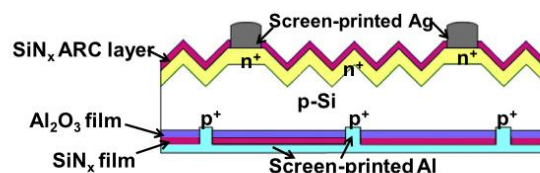


Fig.2. Schematic drawing of the industrial PERC cell structure [7]

The PERC design differs from the conventional full-area rear Al-alloyed BSF. As the recombination of the photo-generated charge carriers at the Al rear contact is only marginally suppressed and the Al layer only partly absorbs infrared light leading to poor light absorption, today's full areal Al-BSF industrial solar cells are limited to around 20% [8]. An important step towards industrialization of the PERC concept was to find a way to obtain low cost and high throughput processes for the deposition of the rear passivation layer.  $\text{SiN}_y$  deposited by PECVD maintained the most promising candidate for a long time, as this technology had already been established as a successful front side passivation layer of phosphorus doped emitter in industrial solar cells. However, as the rear surface is p type, it was discovered that  $\text{SiN}_y$  passivation layers induce an inversion of the surface due to the positive fixed charges within the  $\text{SiN}_y$  layer. This effect was identified by Dauwe et al. in 2002, and parasitic shunting leading to an enhanced carrier recombination was denoted [9].

A rear surface passivation material should have a high fixed negative charge, while at the same time having the ability to provide chemical passivation. Aluminum oxide meets these expectations. Rudolf Hezel and his team from the University of Erlangen-Nuremberg in Germany identified these excellent passivation properties of aluminum oxide back in 1989 [10]. What really makes aluminum oxide so special is its very high density of fixed negative charges of up to  $10^{13}/\text{cm}^3$ . Most of the other passivation films, such as silicon oxide and silicon nitride, have positive fixed charges. With aluminum oxide, the fixed charges are located right

at the interface between aluminum oxide and the interfacial silicon oxide grown on the silicon wafer during the deposition process, which ensures an effective field effect passivation. Aluminum oxide also scores high in chemical passivation. It acts as an effective hydrogen reservoir supplying hydrogen to saturate dangling bonds on the wafer surface during thermal treatment steps. As for the optical properties, these films with a band gap of 6.4 eV are transparent to the portion of sunlight that is relevant to solar cell applications. The only downside is its rather low refractive index of 1.65, which makes aluminum oxide less suitable for being a single layer antireflection film on the emitter side; however, the dielectric very well fulfills the job of back reflector.

## EXPERIMENTS

### *Al-BSF cell fabrication and characterization*

The wafers used for the study were 180–200  $\mu\text{m}$  thick, 2 ohm.cm p-type mc-Si wafers. The wafers were the standard dimensions, 156\*156 mm<sup>2</sup>. Al-BSF mc-Si solar cells were fabricated to study the main properties and parameters.

We produced solar cells with a production feasible process flow outlined in Fig.3.

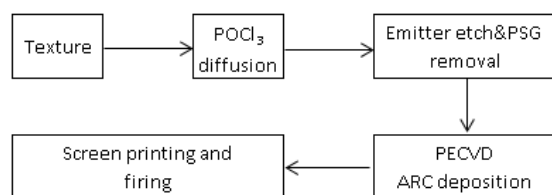


**Fig.3.** Process flow for industrial mc-Si cell fabrication

A solution of hydrochloric and nitric acids (HCl/HNO<sub>3</sub>) was used to texturize the surface of the wafer, resulting in the formation of good textured structure, regardless of the orientation of the crystals. The wafers were treated in a solution of potassium hydroxide (KOH) to etch a layer of porous silicon, then, in order to etch metals, in a solution of hydrofluoric and hydrochloric acids (HF/HCl). The X-Rite SP62 spherical reflectometer was used to measure the reflectivity. Analysis of the surface morphology of silicon wafers before and after texturing was carried out by scanning electron microscopy on a JSM-6390LV microscope.

The emitter was formed using the diffusion method on Lydop equipment from Semco Engineering. Phosphorus doping was carried out at

a pressure slightly below atmospheric and at temperatures of 830–860°C. The phosphorus oxychloride (POCl<sub>3</sub>) was used as a source of phosphorus, which is fed into the reactor along with nitrogen. The emitter, formed at a depth of 0.3–0.5 $\mu\text{m}$ , has two functions: the formation of a p / n junction with the base and the transfer of electrons to metal grid. In order to assess the effect of gettering and measuring the lifetime of minority charge carriers, we used the method of measuring photoconductivity decay in the microwave range ( $\mu$ -PCD) by WT-2000 PVN Semilab measuring system at a laser wavelength of 904 nm.

For the deposition of anti-reflective coating used method of Plasma-Enhanced Chemical Vapor Deposition (PECVD). The deposition of a film of silicon nitride was carried out in a vacuum chamber at a temperature of 350–450°C in the presence of silane (SiH<sub>4</sub>) and ammonia (NH<sub>3</sub>). The thickness of the obtained antireflection coating, measured by Semilab LE-200PV ellipsometer using the polarization-optical method, is around 75 nm.

A metal grid and busbars were applied by screen printing on Dubuit equipment. Silver-containing conductor paste with a specific resistance of less than 2 m $\Omega$ /sq and a viscosity of 16–23 Pa\*s was used for front busbars and grids, and for rear current-collecting pads - silver paste with a resistance of 5 m $\Omega$ /sq and a viscosity of 89 Pa\*s. For applying BSF (backside field), aluminum paste was used, with a resistance of 0.05  $\Omega$ /sq and a viscosity of 50 - 70 Pa\*s.

### *PERC cell fabrication and characterization*

The experiments were performed on diamond sawed mc-Si wafers. The wafers were the standard dimensions, 156\*156 mm<sup>2</sup>. Wafers used for PERC production were gallium doped.

We produced solar cells with a production feasible process flow outlined in Tab.1.

After SDR, wafers were textured and then treated with NaOH solution, creating pyramid-like texture. The front emitter was formed with POCl<sub>3</sub> diffusion. Edge isolation and rear side polishing were performed by a wet chemical process using HNO<sub>3</sub>-HF-H<sub>2</sub>SO<sub>4</sub> solution. The polishing time was 150 second. The rear polished surface will provide better light trapping and passivation opportunities. Polishing is important because if a uniform surface is achieved, this will improve the MACE with respect to homogeneity of the textured surface, and further achieving a well passivated surface with low enough reflectivity. The goal is to achieve smaller and shallower texture on nanoscale, meaning that

pore depth is reduced and pore diameter is decreased.

**Table 1.** Overview of production line

Step
1. Saw damage removal (SDR) and texturing
2. POCl <sub>3</sub> diffusion
3. Wet chemical process of edge isolation and rear side polishing
4. Rear Al <sub>2</sub> O <sub>3</sub> + SiN <sub>y</sub> coating
5. Front PECVD SiN <sub>y</sub> coating
6. Laser ablation (rear contact pattern)
7. Screen printing metallization
8. RTP co-firing

Then the rear side of the cell was passivated by ALD Al<sub>2</sub>O<sub>3</sub>. The passivation layer was deposited by a trimethylaluminium (TMA)-based thermal ALD process, inducing an Al<sub>x</sub>O<sub>y</sub> layer. The post anneal process was implemented in a tube furnace. The thickness of the alumina oxide layer was 14 nm. The annealing time and temperature was 1800 seconds and 520°C. SiN<sub>y</sub> coating was deposited by PECVD, capping the Al<sub>2</sub>O<sub>3</sub>-layer and surfaces were locally patterned using laser ablation. Finally, screen printing and co-firing were used for front and rear side metallization to form front Ag/n+-Si ohmic contact, Al-LBSF and rear local A/p+-Si ohmic contact.

## RESULTS AND DISCUSSION

### Al-BSF solar cells analysis

Fig.4 shows the obtained images of the surface of as cut wafers (Fig.4a), and after texturing (Fig.4b).

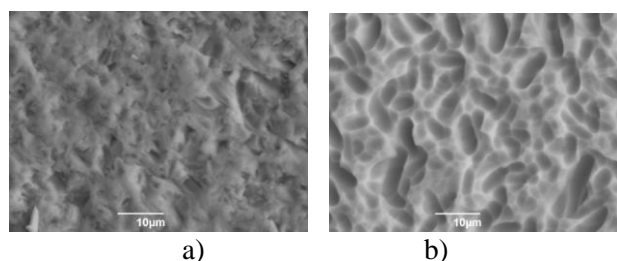


**Fig.4.** SEM - images of the silicon wafer surface: a) as cut; b) after texturing

As Fig.4a shows, the surface of the source wafer was severely damaged. It contains a huge number of cavities, microcracks and hills - this is the disturbed layer that was formed during the wafer production (wire wafer slicing process). Such a surface is simply destructive for the solar cells performance due to the extremely high surface recombination rate. After texturing and etching of

the wafer surface (Fig.4b), wells were formed, which leads to a significant decrease in reflectivity (Fig.5).

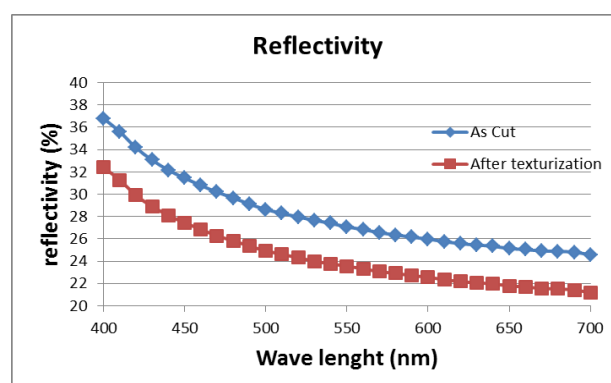


**Fig.5.** The reflectivity of as cut wafers and wafers after texturing, obtained by spherical spectrometry on an X-Rite SP62 reflectometer

In order to assess the effect of gettering, we carried out the study of the lifetime of charge carriers. The measurements were carried out before and after diffusion process. The lifetime mapping of minority charge carriers, as well as average values, was obtained by measuring the photoconductivity decay in the microwave range ( $\mu$ -PCD) on the WT-2000 PVN measuring system. The method of measuring the decay of photoconductivity in the microwave range ( $\mu$ -PCD) is a common method of measuring the lifetime of minority carriers in semiconductors. The method is highly reliable, good reproducibility and speed that provides the possibility of mapping the lifetime of a high-resolution. As the name of the method, it involves the optical excitation and detection of the signal with the microwave system. In this method, a silicon wafer is illuminated by a laser pulse, under the influence of which it generates electron-hole pairs. The transition process of disintegration of the carrier is tracked using a microwave signal. The recombination lifetime is a measure of the quality of the material, that is, the concentration of defects /impurities, which affects the quality of the resulting detectors and their electrical properties.  $\mu$ PCD – non-destructive testing contactless method, which allows to map the recombination lifetime of the wafer as a whole to its selection for processing in order to obtain devices/detectors.

The study showed that the lifetime of charge carriers increased from 2  $\mu$ s (before the diffusion process) to 11.6  $\mu$ s (with a formed emitter after diffusion) (Fig.6). The trend shows the effect of gettering by diffusion.

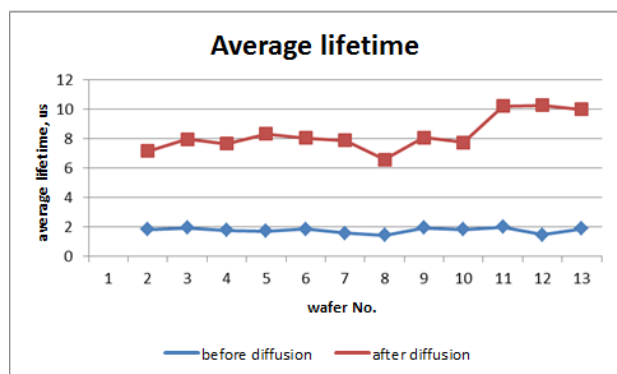


Fig.6. Lifetime trend

As can be seen in Fig.7, the lifetime is distributed more evenly, with the exception of the boundary zones, where an accumulation of lattice defects and recombination zones formed during the crystallization process occurred. It is known [12-15], that the surface of mc-Si wafer is a maximum possible disorder in the crystal lattice symmetry, resulting in increased surface recombination of charge carriers.

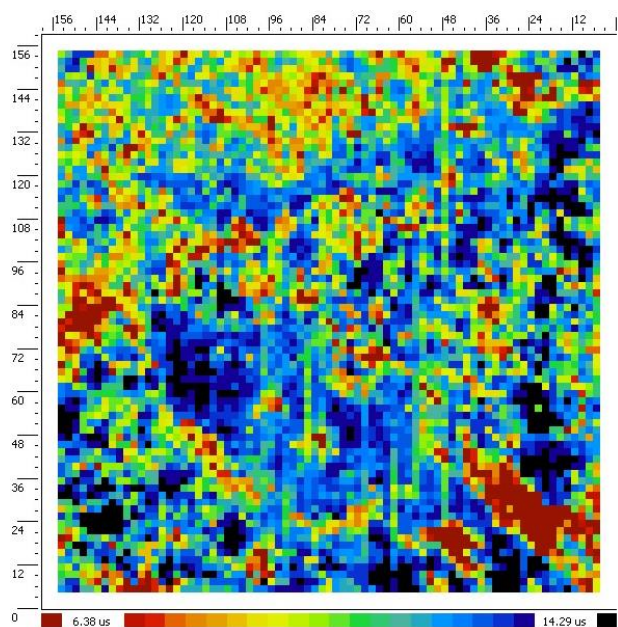


Fig.7. Lifetime Semilab map (scale 6.38-14.29 μs). average: 11.293 μs median: 11.89 μs deviation: 22.545% min: 2.16 μs max: 15.788 μs

Surface recombination can greatly affect the  $I_{sc}$  and  $V_{oc}$ . Surface recombination has a particularly detrimental effect on the short-circuit current ( $I_{sc}$ ), since the front surface is also the region with the highest carrier generation in the solar cell. The reduction of high surface recombination is usually achieved by reducing the number of dangling bonds on the surface by passivating it. In this work, the surface was passivated using non-stoichiometric films with a large amount of hydrogen ( $Si_xN_y: H$ )

applied using the PECVD method. We used an ellipsometer Semilab LE 200PV to measure the thickness and refractive index of the films obtained. The refractive index is 2.05-2.06, and the thickness of the films obtained varies from 73 to 78 nm.

The study of the properties and parameters of silicon wafers and solar cells by the method of spectrometric analysis of photoluminescence was carried out at the National Institute of Solar Energy of France (INES). PL images of silicon wafers (Fig.8) and fabricated solar cells (Fig.9) were obtained by Luminescence Imaging System - Model LIS-R1.

The dark zones present in the PL images of silicon wafers (Fig.8) can be the sites of dislocation accumulations that occur during the crystallization of silicon ingots. These defects adversely affect the performance of solar cells.

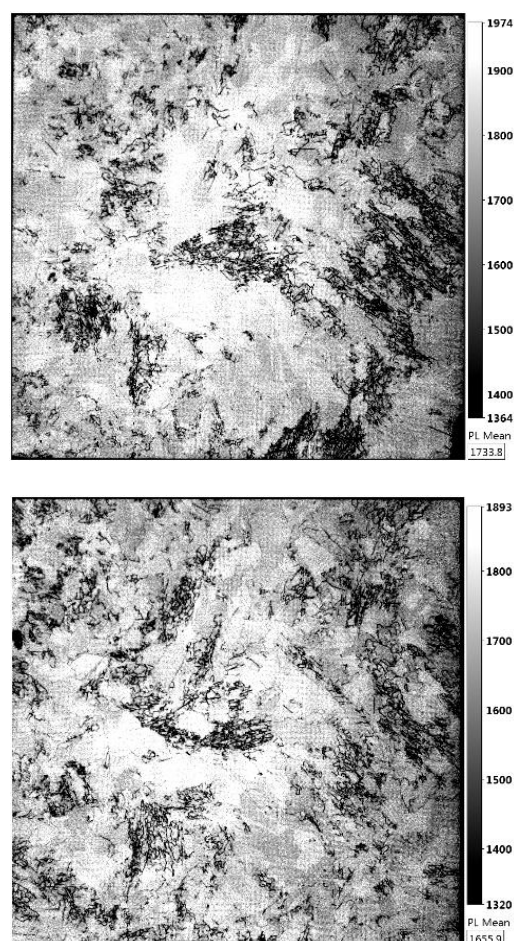


Fig.8. PL images of silicon wafers (samples 1, 10)

Analysis of the obtained PL images of solar cells (Fig.9) proved the assumption that the dark zones are the result of the accumulation of defects arising in the process of crystallization and do not occur as a result of the production of solar cells.

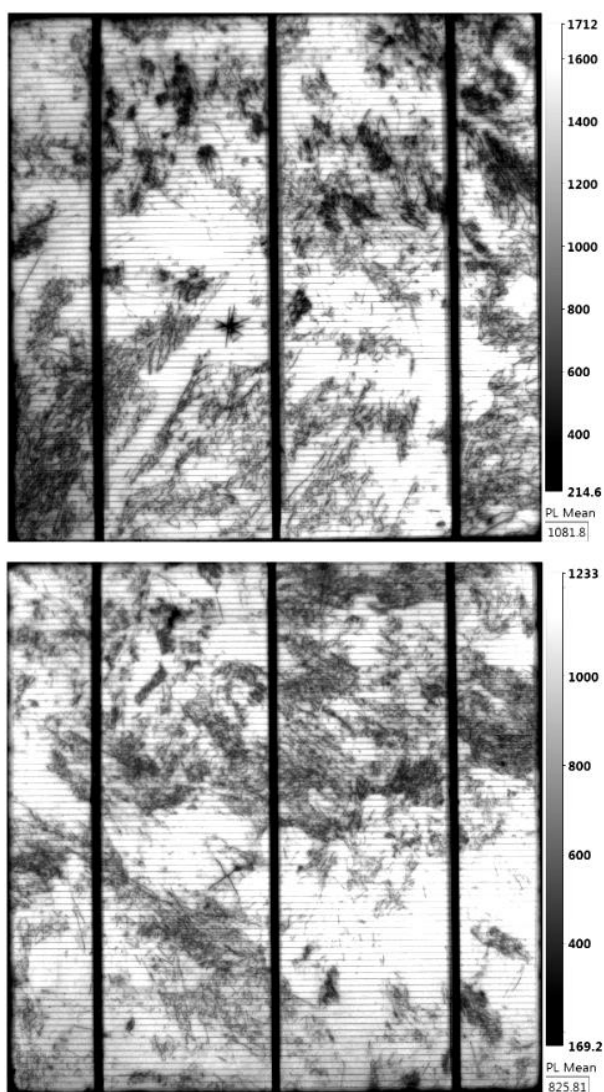


Fig.9. PL images of solar cells (samples 1, 10)

To measure the electrical parameters (current-voltage curves) (Isc short-circuit current, open circuit voltage Uoc, filling factor FF, maximum power Pmpp, efficiency), the Solar simulator ORIEL Sol3A CLASS AAA was used. The measurement results and the obtained current – voltage curves are presented in Tab.2 and in Fig.10.

Table 2. Electrical performance of Al-BSF solar cells

No.	Voc mV	Isc A	FF %	Rsh $\Omega$	Eff %
400	610.3	8.5	76.80	102.3	15.83

Thus, the studied samples of solar cells of Kazakhstan production showed efficiency in the range from 15.6 ÷ 15.9%. Kazakhstan Solar Silicon LLP production requires an upgrade and process tuning.

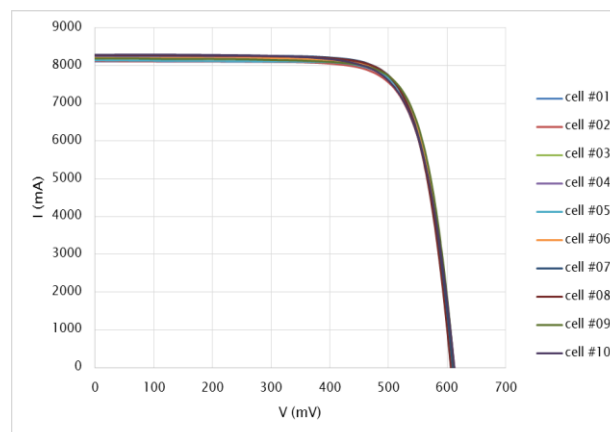


Fig.10. Current - voltage curves

### PERC solar cells analysis

The results of PERC cells are presented in Tab. 3. An approximate average of the efficiency of all PERC solar cells is 19.78%.

Table 3. Electrical performance of PERC solar cells

No.	Voc mV	Isc A	FF %	Rsh $\Omega$	Eff %
400	650	9.42	79.30	276.1	19.89

Internal quantum efficiency (IQE) is given in Fig.11. Measurement of short-circuit current in the external quantum efficiency was obtained on the Semilab WT-2000 PVN measuring system. The method is based on the principle of light a very small area of the solar cell with a laser beam that is focused directly on the surface of the solar cell. IQE is the ratio of the number of charge carriers collected by the solar cell to the number of photons of a given energy that shine on the solar cell from outside and are absorbed by the cell. It can be observed that the collection of carriers is higher for the optimized PERC by about 900-1000 nm. This is consistent with the literature, as the introduction of  $Al_2O_3$  has been found to improve the optical reflectivity at the rear of the cell, and thereby to increase the absorption due to improved light-trapping, especially in the IR light region (700-1000 nm).

An important loss mechanism for PERC is bulk recombination. A possible solution to overcome this is to improve the phosphorus diffusion gettering, which can be done by optimizing the emitter doping process.

Further improvement of the PERC production line is necessary to reach the 24% limit. PERC design requires a finetuning of influencing parameters that are not linearly interrelated, thus it is a complicated matter to investigate.

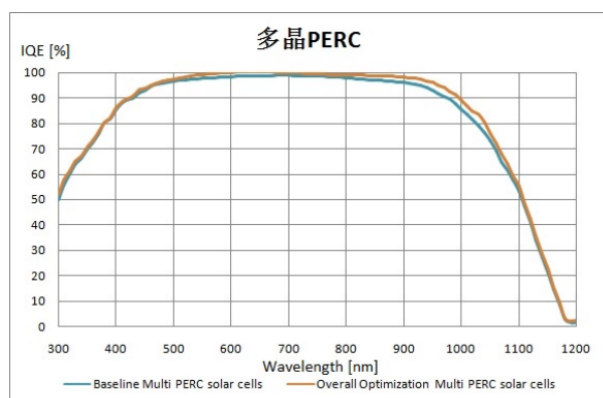


Fig.11. Internal quantum efficiency

*Upgrade of standard line to PERC*

Processing PERC involves depositing a rear surface passivation film, which is subsequently opened to give way for formation of a rear contact – these are two important additional steps over in Kazakhstan solar cell processing (Fig.12).

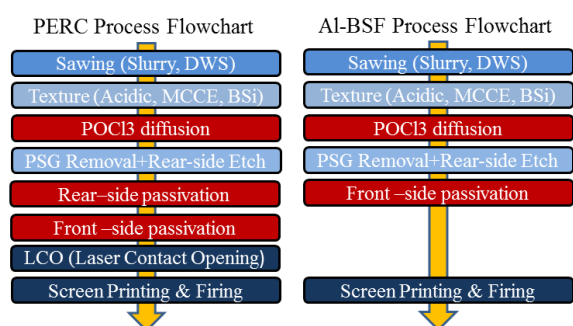


Fig.12. Process sequences for Production of PERC cells

In addition, the chemical wet-bench based edge isolation step is tweaked for rear polishing. That means texturing accomplished on both sides of the wafer is removed only on the rear side by etching off the pyramid structure. The degree of polishing changes from case to case. Thus, a passivation film deposition system and a film opening system - mainly accomplished with PECVD and lasers - are additional tool sets typically hooked up to standard cell processing lines.

A cell line for PERC technology requires only two pieces of additional equipment compared to a standard line – devices for rear passivation and laser structuring. This means upgrades to PERC are simple.

Kazakhstan Solar Silicon LLP has equipment for anti-reflective coating (silicon nitride) deposition TWYN PECVD. The PECVD process consists of the decomposition of a chemical element under the influence of plasma and temperature into individual elements in the reactor,

which then settle to the surface of the wafer and enter a chemical reaction. As a result, the film (up to 80 nm) of silicon nitride, which has the required properties, is “grown” on the front surface of the wafer. PECVD equipment can be modified to apply a rear passivation layer (AlOx + SixNy), while the general principle of deposition remains the same. Introducing a trimethylaluminum (TMA) precursor and adaption of the cleaning mechanism are more or less the two main fundamental changes that PECVD systems are required to undergo to be able to apply aluminum oxide films on the rear side of the cell. Not only the generic deposition principle of PECVD stays the same, which is the radio frequency (RF) power used to dissociate precursors at low pressure and which leads to depositing the required film on the substrate present in the chamber. Even the equipment makers’ proprietary plasma generating mechanisms do not need to be changed. One inherent advantage of PECVD systems over ALD tools is the capability to deposit the silicon nitride capping layer on top of aluminum oxide in one system without breaking the vacuum. That means the complete rear passivation process is executed in one pass.

The easiest way to open the rear passivating layer is to utilize laser technology. This step is generally called laser contact opening (LCO). Today, the photovoltaic industry has a large number of laser solutions offered by companies such as InnoLas Solutions, Rofin, 3D-Micromac, Schmid or Manz.

Like any other advanced cell technology, PERC requires a special metallization paste system. The most critical metallization product is a BSF paste. A suitable aluminum paste does not react on those areas where it covers the passivation layer, but at the same time it establishes contacts at areas opened with lasers to create a local BSF. A nonreactive rear tabbing silver paste is required as well. The attributes for such pastes are twofold: It should not fire through the passivation layer and it should exhibit good adhesion and solderability. Technically speaking, only special rear tabbing and BSF pastes are required for PERC cells, while the standard front contacting paste can be applied on the emitter side as well. However, taking into consideration the fact that PERC cells need to be processed at relatively low temperatures, paste suppliers are also promoting dedicated front contacting paste for this technology. The local BSF can be implemented in many ways. The standard is to have the laser contact opening the line pattern. There is potential to improve efficiency when a dot

or dashed pattern is applied for rear passivation stack opening. This reduces bulk resistivity of the rear contact as the silver paste is not spread all over. Toyo is offering such special aluminum pastes. The company is using silicon doped aluminum pastes which facilitate alloy formation during rear contact realization, thereby improving effectiveness of contact formation. There is another important improvement in the PERC segment, as the first cell manufacturers are working on having aluminum oxide on both sides of the wafer. Adding aluminum oxide on the emitter side requires paste optimization, as the paste has to penetrate through an extra layer of dielectric film.

## CONCLUSIONS

The results based on all experiments were combined to investigate the total effect of the upgrading of production line. The results are presented in Tab. 4. It is possible to observe that the upgrade of standard line to PERC was successful, and a champion efficiency above 19% achieved.

Further improvement of the PERC production line is necessary to reach the 24% limit. PERC design requires a finetuning of influencing parameters that are not linearly interrelated.

**Table 4.** Cell performance of Al-BSF and PERC solar cells based on Kazakhstan Silicon

Group	Voc mV	Isc A	FF %	Rsh $\Omega$	Eff %
PERC	650	9.42	79.30	276.1	19.89
Al-BSF	610.3	8.5	76.80	102.3	15.83

At Kazakhstan Solar Silicon LLP it is possible to switch from Al-BSF standard solar cell production line to the PERC line, which will allow the company to increase the efficiency of the produced solar cells and be competitive in the global market.

## REFERENCES

- [1] Department of Economic and Social Affairs. World population prospects: *The 2018 revision*.
- [2] US Energy Information Administration. *International energy outlook 2018*, (2018).
- [3] K. Murukesan, S. Kumbhar, A. K. Kapoor, A. Dhau, S. Saravanan, R. Pinto, B. M. Arora. POCl diffusion process optimization for the formation of emitters in the crystalline silicon solar cells. *IEEE 40th PV Specialists conf. IEEE*, (2014).
- [4] Martin A Green. *Solar cells: operating principles, technology and system applications*, 1992.
- [5] Jenny Nelson. *The physics of solar cells*. Imperial College Press, London, 2003.
- [6] Matthias Byungsul Min, Hannes Muller, Gerd Wagner, Rolf Fischer, Pietro P. Brendel, Holger Altermatt, and Holger Neuhaus. A roadmap toward 24% efficient perc solar cells in industrial mass production. *Photovoltaics, IEEE Journal of*, **7 (6)**, 1541–1550, (2017).
- [7] Haibing Huang, Jun Lv, Yameng Bao, Rongwei Xuan, Shenghua Sun, Sami Sneek, Shuo Li, Chiara Modanese, Hele Savin, Aihua Wang, and Jianhua Zhao. 20.8 efficiency loss mechanisms analysis and roadmap to 24. *Solar Energy Materials and Solar Cells*, **161**, 14–30, (2017).
- [8] Thorsten Dullweber and Jan Schmidt. Industrial silicon solar cells applying the passivated emitter and rear cell (perc) concept, review. *Photovoltaics, IEEE Journal of*, **6 (5)**, 1366–1381, (2016).
- [9] S. Dauwe, L. Mittelstädt, A. Metz, R. Hezel. Exp. evidence of parasitic shunting in silicon nitride rear surface passivated solar cells. *Progress in PV: Research and Appl.*, **10 (4)**, 271–278, (2002).
- [10] R. Hezel, K. Jaeger Low-Temperature Surface Passivation of Silicon for Solar Cells Solid-State Science and Technology - *TECHNICAL PAPERS J. Electrochem. Soc.* **136 (2)**, 518-523 (1989).
- [11] D. Schroder, Semiconductor material and device characterization, *3rd edition ed. Piscataway NJ; Hoboken N.J.: IEEE Press; Wiley*, (2006).
- [12] Jan Schmidt, Robby Peibst, Rolf Brendela Surface passivation of crystalline silicon solar cells: Present and future. *Solar Energy Materials and Solar Cells* **187**, 39-54 (2018).
- [13] Jae Eun Kim, Se Jin Park, Ji Yeon Hyun, Hyomin Park, Soohyun Bae, Kwang-sun Ji Hyunho, Kim Kyung Dong Lee, Yoonmook Kang, Hae-Seok Lee, Donghwan Kim Characterization of SiNx:H thin film as a hydrogen passivation layer for silicon solar cells with passivated contacts. *Thin Solid Films* (2019).
- [14] J. A. Silva, A. Lukianov, R. Bazinette, D. Blanc-Pélissier, Julien Vallade, Sylvain Pouliquen, Laura Gaudy, Mustapha Lemiti, Françoise Massines Feasibility of Antireflection and Passivation Coatings by Atmospheric Pressure PECVD. *Energy Procedia* **55**, 741-749 (2014).
- [15] L. E. Blacka, B. W. H. van de Loo, B. Macco, J. Melskens, W. J. H. Berghuis, W. M. M. Kessels Explorative studies of novel silicon surface passivation materials: Considerations and lessons learned. *Solar Energy Materials and Solar Cells* **188**, 182-189 (2018).
- [16] S. Plotnikov, D. Kalygulov, I. Klinovitskaya Research of the production technology of photovoltaic cells. *Bulletin D. Serikbayev EKSTU* **4 (78)**, 67-73 (2017).